

Finite-Element Modeling of a Fighter Aircraft Canopy Acrylic Panel

John J. Labra*

Southwest Research Institute, San Antonio, Tex.

A detailed three-dimensional stress analysis of a canopy aircraft acrylic panel was conducted to investigate the probable cause of a recent in-flight acrylic panel failure. The analysis was made using a general-purpose finite-element computer program. Based in part on this analysis, probable design problems associated with the canopy were identified. The study clearly demonstrates that computer-based technology can be successfully used in determining probable causes of failure in geometrically complex structures.

Introduction

TYPICAL military aircraft undergo variable stresses during in-flight operations which are caused, in part, by a pressure differential between the interior and exterior of the canopy, as well as by transient forces imposed during aircraft military high-speed maneuvering operations. Recently, during in-flight maneuvers, an Air Force fighter aircraft experienced a canopy acrylic panel failure. To date, the research to delineate the cause of failure has primarily been experimental. This has involved pressure testing of canopies as well as an in-depth material analysis of acrylic specimens taken from the fractured canopy panel. Preliminary findings suggest that failure was caused by a crack originating in the right rear corner region of the canopy (Fig. 1). The crack is believed to have resulted from concentrated stresses on the rearmost right corner node of the canopy; these stresses resulting from internal pressure, external side loads (during flight), temperature, and/or preloads inherent to the structural design, fabrication, and assembly of the canopy.

The canopy consists of a one-piece biaxially stretched acrylic (methyl methacrylate, per MIL-P-25690A) panel attached longitudinally to the aircraft side beams by a piano hinge system (Fig. 2). The canopy forward and aft supports (Fig. 1) are an extruded aluminum arch and a builtup arch, respectively. Since failure occurred while the canopy was closed, emphasis was placed on investigating the canopy loading environment and in-flight performance while in the closed mode.

With the canopy closed, there are two critical design conditions. They entail a uniform ground pressurization testing requirement and a nonsymmetric load condition. The ground pressurization criterion¹ involves a uniform pressure distribution applied internally (acting outward) on the canopy. The test or design pressure is 69 kPa (10 psi). The nonsymmetrical load distribution criterion is representative of an imposed loading on a canopy during flight operations with the aircraft maintaining a zero angle of attack, a 1 deg side slip, and a speed of Mach 1.07. For this nonsymmetrical loading (acting outward), a maximum 53 kPa (7.7 psi) pressure is applied at the canopy-type centerline.

During the development of the particular aircraft, the canopy was analyzed for the unsymmetrical loading condition by modeling the canopy as a series of annular arches. The arches were pin-ended at the canopy side beams and the applied loading was based on the average external pressure imposed on the canopy between 127 and 508 mm (5 and 20 in.) behind the forward arch support (Fig. 3). This approach

is reasonable for those areas away from the forward or rear arch supports. The validity becomes questionable for regions in the extreme forward or rear locations of the canopy. These localized forward and aft regions are, however, of concern because of the recent in-flight failure.

From the foregoing discussion, it is evident that the loading environment and the geometry of the canopy are quite complex. The purpose of the present paper is to study the load response of the entire canopy as a single entity and to demonstrate that computer-based technology can be used successfully to delineate probable causes of failure to complex structures.

Finite-Element Model

To investigate the ground pressurization and in-flight response of a closed canopy, the acrylic panel was modeled using the MARC general-purpose finite-element computer program.² Since the panel thickness-to-radii ratio is approximately 0.014, a thin-shell analysis is acceptable. The analysis was handled using isoparametric curved triangular shell elements to model the acrylic. The shell nodal points were first defined in a surface Gaussian coordinate system. These points were then mapped into a three-dimensional Cartesian coordinate system. This entailed developing regression formulas which related the spacial coordinates with the Gaussian coordinates. These formulas were based, in part, on data supplied by the U.S. Air Force.

Two mesh configurations of the canopy were constructed. Model A (Fig. 4) consists of 72 elements, 49 nodal points, and 441 degrees of freedom (Table 1). The degrees of freedom are defined in terms of the spacial (Cartesian) components of displacement u , v , and w and the rates of change with respect to the Gaussian coordinates. The second configuration (model B) consists of a finer mesh (Fig. 5) and includes 128 shell elements, 81 node points, with a corresponding 729 unrestrained degrees of freedom. Since the approximations inherent with finite-element theory involve the physical model, the latter mesh was warranted to ascertain the validity of results with the coarser grid.

The acrylic was assumed to behave as an isotropic, elastic-plastic material with a Mises yield criterion. This criterion states that first yield occurs when the effective stress $\bar{\sigma}$ equals the yield stress σ_y of the material based on a uniaxial test. A yield stress σ_y of 6.2 MPa (9000 psi), modulus of elasticity E of 293 MPa (4.25×10^5 psi), and an acrylic thickness of 5.8 mm (0.23 in.) were used for all the simulations. The thickness is typical of the aircraft canopy and the yield stress is the minimum specification of methyl methacrylate. The elastic-plastic analysis entailed specifying three equal layers through the thickness of the acrylic for which integration is performed using Simpson's rule. For each element, integration is performed by the MARC program at seven points per layer.

Received May 21, 1980; revision received Aug. 13, 1981. Copyright © American Institute of Aeronautics and Astronautics, Inc., 1981. All rights reserved.

*Senior Research Scientist.

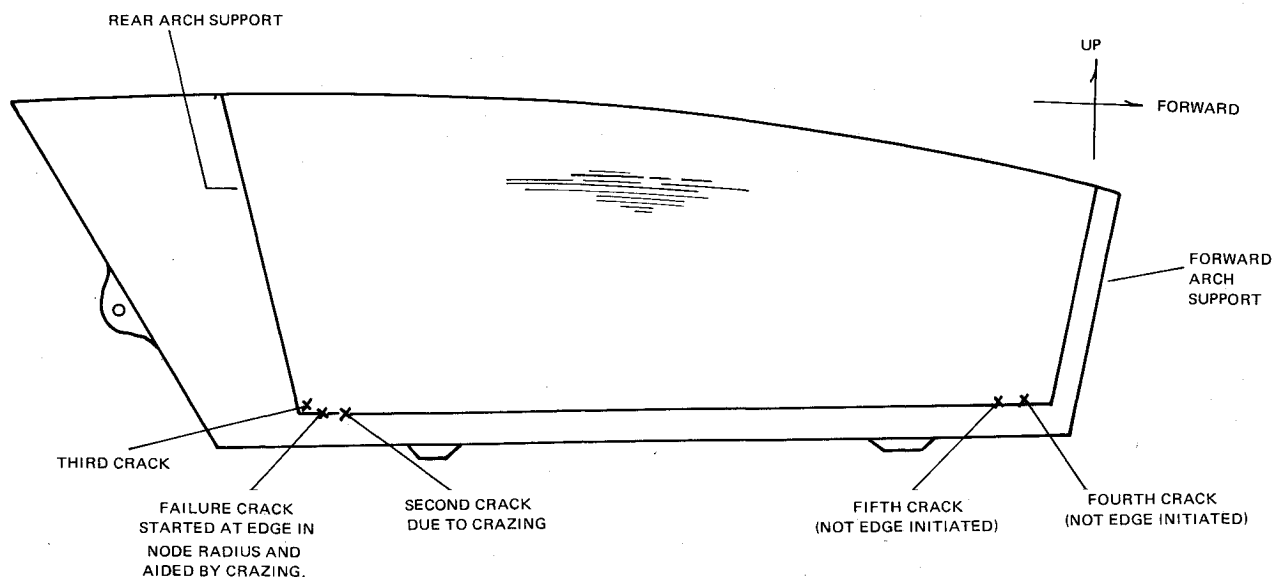


Fig. 1 General location of cracks found on failed acrylic panel.¹

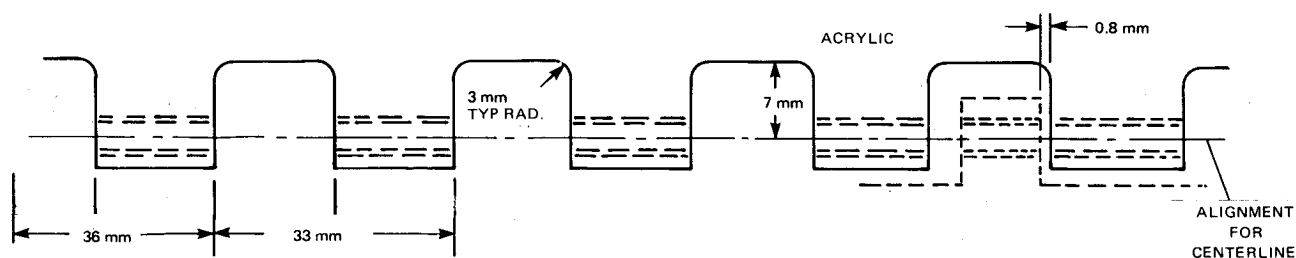


Fig. 2 Acrylic panel hinge node spacing, side-beam location.

Loading and Boundary Conditions

Two loading conditions were considered in the present investigation. A uniform pressure distribution acting outward was imposed to investigate the canopy response to a typical ground pressurization mode.¹ For an in-flight loading environment, a nonsymmetrical loading was imposed.

The nonsymmetrical pressure distribution was assumed to vary only along the circumference of the canopy and be independent of the longitudinal (fore-aft) direction. This is similar to past design approaches (Fig. 3) using annual arch theory.

Since boundary conditions may have a significant effect on the load-carrying capacity of the acrylic, various boundary configurations were considered and are described in Table 2. Based on available data as well as testing performed at SwRI, constraint classification I best simulates the actual support conditions for the canopy in its closed mode. With constraint type I, the acrylic model was free to expand or contract longitudinally at the forward and rear arch support locations. Rotational degrees of freedom were included, excluding those which would induce warping at each arch support. The supports representative of the aircraft side beams permitted only rotation about each respective longitudinal axis.

Constraint classifications II-IV were used in limited simulations to evaluate the sensitivity of constraint variations on the ultimate response of the canopy panel. In particular, classes III and IV are unrealistic in terms of being representative of the physical attachments of the panel to the aircraft structural canopy assembly.

Simulation Results

To investigate the fighter aircraft canopy performance during operational conditions, simulations encompassed two basic categories; the first assumed imposed loading due solely

to pressure applied to the acrylic panel, while the second considered the possibility of prestressing along the boundary's representative of the aircraft side beams as well as the loadings considered in the first category. For both situations, uniform and nonsymmetrical pressure distributions were applied to the acrylic.

Nonprestress Conditions

Six nonprestress simulations were made of canopy response to pressure loadings. Five involved a uniform pressure configuration (cases 2-6) and one considered a nonsymmetrical loading. As illustrated in Table 3, the repetitive cases (3-6) with the uniform pressure mode were made to evaluate the postload performance of the canopy to prescribed variations in the boundary conditions and to ascertain a level of confidence concerning the coarser grid model A. With the critical pressure defined as that resulting in elastic-plastic yielding of the acrylic, only a minor change in ultimate pressure occurred when the uniform load condition (case 2) was repeated with the finer mesh (model B). As a result, all additional simulations involved using model A.

For all of the simulations, the critical pressure far exceeded the design uniform and nonuniform pressure distributions. With prescribed boundary conditions reflective of the actual canopy (case 2), the failure load was 317 kPa (46 psi) under the uniform pressure condition. This exceeds the ground pressurization requirement by a factor greater than 4. With the nonsymmetrical loading (case 1), material yielding occurred only when the pressure distribution was magnified by a factor of over 7.

In both cases (1 and 2), failure occurred adjacent to the piano hinge between 0.5 and 0.7 m (18 and 27 in.) behind the forward arch. In the nonuniform pressure simulation, the failure occurred along the left side of the canopy. The uniform pressure failure occurred simultaneously at

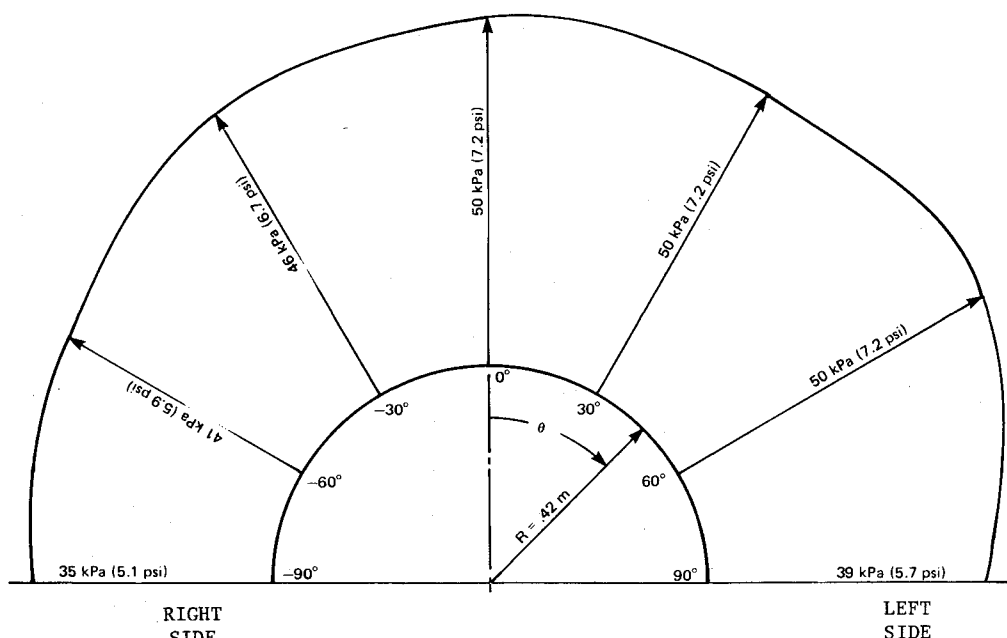


Fig. 3 Nonuniform pressure.

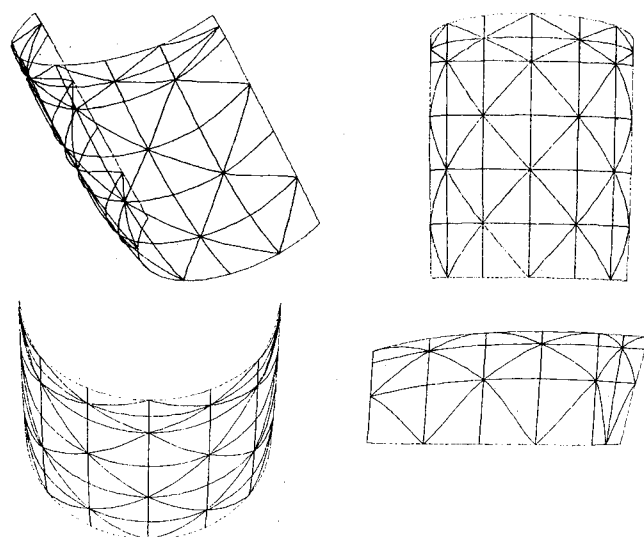


Fig. 4 Coarse mesh model.

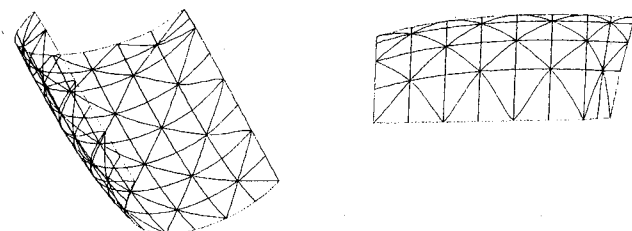


Fig. 5 Fine mesh model.

corresponding locations on both right and left sides of the canopy adjacent to the side beam supports.

Prestress Conditions

The findings given in Table 3 are based on the ideal canopy panel attachment conditions. No consideration is given to potential preloads due to design or mounting procedures associated with the aircraft canopy. In particular, it is assumed that the mating of the aircraft side-beam nodes with the acrylic panel nodes (Fig. 2) by means of an alignment pin

Table 1 Finite-element canopy models

Designation	No. of elements	No. of node points	No. of DOF ^a
A	72	49	441
B	128	81	729

^a Unrestrained degrees of freedom.

do not result in prestressing of the acrylic. X-ray data supplied by the Air Force, however, suggest that prestressing of the acrylic exists due to local deformation of the alignment pin or to interaction of adjacent side-beam/acrylic nodes. While the magnitude of these loads has not been quantified, the sensitivity of the critical pressure to localized deformation due to canopy/side-beam prestressing was investigated.

Seven simulations were performed with the acrylic panel undergoing localized deformations prior to imposing either uniform or nonuniform pressure distributions. Arbitrarily picked, the preload deformation was limited to a single point approximately 0.7 m (26 in.) from the forward arch either along the right or left boundary representing the acrylic panel/side-beam interface. Table 4 summarizes the findings from these simulations.

Bidirectional Deformation

In case 7, along the right-side acrylic panel/side-beam interface, a lateral inboard and vertical downward displacement of 1.3 mm (0.050 in.) resulted in acrylic yielding under a uniform pressure of 31 kPa (4.47 psi). Reducing this deformation to 0.6 mm (0.025 in.) (case 8) resulted in a critical pressure of 61 kPa (8.92 psi). In comparison, the early case 2 simulation (Table 2) demonstrated an ultimate pressure of 317 kPa (46.0 psi).

Case 9 is a repeat of case 8 with the nonsymmetrical pressure condition imposed (Fig. 3). As given in Table 4, the acrylic panel ultimate stress occurred when the pressure reached 89% of the specified in-flight design criterion. This is a significant reduction over the nonprestress state (case 1) where material first yield occurred at 730% of design pressure.

Case 10 is a repeat of the nonsymmetrical load case 9 except that the preload deformation is located at the corresponding acrylic panel/side-beam interface on the left side of the aircraft. No significant change in critical pressure occurred.

Table 2 Canopy constraint summary

Simulation case no.	Constraint classification no.	Summary
1-3,7-12	I	Canopy allowed to rotate about longitudinal axis representing side-beam piano hinges. This precludes translational motion (unless prescribed). Forward and aft arch supports permit longitudinal displacement and rotation excluding warping along arch periphery.
4	II	In addition to constraints imposed in cases 1-3, 7-12, rear arch constraint imposed preventing longitudinal displacement.
5	III	Constraints imposed along piano hinges limited to translational (warping along hinge lines permitted).
6	IV	Constraints along piano hinges as specified in case 5. In addition, rotational constraints along forward and rear arch peripheries removed (allowing warping).

Table 3 Nonprestress canopy simulation summary

Case no.	Model	Load type	Boundary classification ^a	Critical pressure, kPa (psi) ^b
1	A	Nonsym.	I	7.3 ^c
2	A	Sym.	I	317 (46.0)
3	B	Sym.	I	312 (45.3)
4	A	Sym.	II	316 (45.8)
5	A	Sym.	III	272 (39.5)
6	A	Sym.	IV	267 (38.8)

^aSee Table 2. ^bAcrylic first yield based on Mises yield criterion. ^cFor nonsymmetrical loading, critical pressure is given in terms of multiple of design criterion.

Table 4 Prestress canopy simulation summary

Case no.	Model	Constraint class.	Type loading	Preload displacement data			Critical pressure, kPa (psi)
				Location ^a	Direction ^b	Magnitude, mm	
7	A	I	Sym.	RPH/0.7	<i>u/w</i>	-1.3/-1.3	31 (4.47)
8	A	I	Sym.	RPH/0.7	<i>u/w</i>	-0.6/-0.6	61 (8.92)
9	A	I	Nonsym.	RPH/0.7	<i>u/w</i>	-0.6/-0.6	0.89 ^c
10	A	I	Nonsym.	LPH/0.7	<i>u/w</i>	-0.6/-0.6	0.89
11	A	I	Nonsym.	LPH/0.7	<i>w</i>	-0.6	0.75
12	A	I	Nonsym.	LPH/0.7	<i>u</i>	-0.6	2.96
13	A	I	Nonsym.	LPH/0.7	<i>v</i>	+0.6	0.53

^aRPH = right-side piano hinge; integer is distance (m) along side beam behind forward arch support; LPH = left-side piano hinge. ^b*u* = lateral direction (positive outboard, negative inboard); *v* = longitudinal direction (positive rearward); *w* = vertical direction (positive upward). ^cFor nonsymmetric load cases number is multiple of inflight design criterion.

Unidirectional Deformation

The last three simulations were made to determine which potential misalignment or interference fit direction is most critical in terms of ultimate pressure. For all cases (11-13), the nonsymmetrical load distribution shown in Fig. 3 was used. As in case 10, a preload deformation of 0.6 mm (0.025 in.) was located along the left-side acrylic panel/side-beam interface 0.7 m (26 in.) behind the forward arch support. As shown in Table 4, the lowest critical pressure occurred when the preload displacement is limited to the longitudinal *v* direction (case 13). In this instance, acrylic plasticity occurred at a pressure 53% of the nonsymmetric load design criterion. The smallest reduction in ultimate pressure occurred in case 12 where the preload deformation was in the lateral inboard direction. Here, the acrylic yielded at a pressure 2.96 times the design criterion for nonsymmetrical loadings, still a substantial reduction in the safety margin associated with the canopy under ideal nonprestress conditions.

It is also noted, as with the nonprestress simulations, the critical regions are in the vicinity of the acrylic panel/side-beam boundaries. Further, irrespective of whether the

nonsymmetric loading was directed toward or away from the preload deformation, failure occurred at approximately the same load level (cases 9 and 10) and in the vicinity of the preload localized deformation. This further suggests an extreme sensitivity of prestressing on the acrylic panel inflight response.

Conclusions

A general-purpose finite-element computer program has been used to identify the probable cause of failure of a fighter aircraft canopy acrylic panel. Pertinent findings from this investigation are:

1) Under ideal (nonprestress) conditions the canopy acrylic panel can withstand significant uniform and nonuniform pressures well beyond those specified as design criteria. Uniform pressure loadings as high as 317 kPa (46 psi) were simulated before acrylic material yielding occurred.

2) The aircraft canopy acrylic panel load-carrying capacity is extremely sensitive to prestressing and/or localized deformation due to misalignment along the acrylic panel/side-beam interfaces. In certain simulations, plastic

yielding of the acrylic occurred well below the uniform design pressure criterion of 69 kPa (10 psi). This same sensitivity was reflected in simulation results for the acrylic panel exposed to nonuniform pressure distributions.

3) Fore-aft deformation along an acrylic panel/side-beam piano hinge presents the greater risk in comparison with similar localized deformations in either vertical or lateral directions.

4) While the degree of prestressing has yet to be quantified, available x-ray data of acrylic panel/side-beam node interference and/or alignment pin deformation have shown that prestressing of the acrylic occurs. Based on the simulation

findings and the x-ray data, a situation could result with the canopy acrylic panel failing under either ground or in-flight conditions. A nondestructive inspection program would, however, reduce the probability of such an incident.

References

¹"Military Specification Structural Criteria, Airplane Strength and Rigidity Loads," MIL 8861, May 18, 1960.

²"MARC-CDC General Purpose Finite Element Analysis Program," Vols. I, II, and III, Rev. K, Control Data Corp., Minneapolis, Minn., Nov. 1979.

From the AIAA Progress in Astronautics and Aeronautics Series . . .

COMBUSTION EXPERIMENTS IN A ZERO-GRAVITY LABORATORY—v. 73

Edited by Thomas H. Cochran, NASA Lewis Research Center

Scientists throughout the world are eagerly awaiting the new opportunities for scientific research that will be available with the advent of the U.S. Space Shuttle. One of the many types of payloads envisioned for placement in earth orbit is a space laboratory which would be carried into space by the Orbiter and equipped for carrying out selected scientific experiments. Testing would be conducted by trained scientist-astronauts on board in cooperation with research scientists on the ground who would have conceived and planned the experiments. The U.S. National Aeronautics and Space Administration (NASA) plans to invite the scientific community on a broad national and international scale to participate in utilizing Spacelab for scientific research. Described in this volume are some of the basic experiments in combustion which are being considered for eventual study in Spacelab. Similar initial planning is underway under NASA sponsorship in other fields—fluid mechanics, materials science, large structures, etc. It is the intention of AIAA, in publishing this volume on combustion-in-zero-gravity, to stimulate, by illustrative example, new thought on kinds of basic experiments which might be usefully performed in the unique environment to be provided by Spacelab, i.e., long-term zero gravity, unimpeded solar radiation, ultra-high vacuum, fast pump-out rates, intense far-ultraviolet radiation, very clear optical conditions, unlimited outside dimensions, etc. It is our hope that the volume will be studied by potential investigators in many fields, not only combustion science, to see what new ideas may emerge in both fundamental and applied science, and to take advantage of the new laboratory possibilities.

280 pp., 6×9, illus., \$20.00 Mem., \$35.00 List

TO ORDER WRITE: Publications Dept., AIAA, 1290 Avenue of the Americas, New York, N.Y. 10104